EFFECTS OF SOIL NON-LINEARITY ON THE SEISMIC DISTRESS OF RETAINING WALLS

Y. Tsompanakis[1] and P. N. Psarropoulos[2]

[1] *Asst. Professor, Dept. of Applied Sciences, Technical University of Crete, Crete, Greece*
[2] *Lecturer, Dept. of Infrastructure Engineering, Hellenic Air-Force Academy, Athens, Greece*
Email: jt@science.tuc.gr, prod@central.ntua.gr

ABSTRACT :

Despite the structural simplicity of retaining walls, their seismic response is a rather complicated problem. What makes that response so complicated is the dynamic interaction between the wall and the retained soil, especially when material and/or geometry non-linearities are present. This paper aims to examine how and to what extent the potential soil non-linearity may affect both the dynamic behavior of a rigid non-sliding retaining wall and also the seismic response of the retained soil layer. For this purpose an extensive parametric study, based on two-dimensional dynamic finite-element analyses, is conducted. Soil non-linearity is realistically taken into account via a computationally efficient equivalent-linear procedure. The examined numerical model is studied under different excitations and various levels of the imposed ground motion maximum accelerations to examine more thoroughly the influence of material non-linearity. The results of this study justify the hypothesis that the non-linear soil behavior has a considerable impact not only on the dynamic earth pressures developed on the wall, but on the amplification of the acceleration levels on the backfill soil as well. Therefore, it becomes evident that seismic codes and geotechnical design practice should take this impact into serious consideration.

KEYWORDS: retaining walls, dynamic response, soil non-linearity, amplification, dynamic SSI

1. INTRODUCTION

Undoubtedly, retaining walls have many applications in geotechnical engineering practice. Harbor quay-walls, bridge abutments, or deep excavations are some of the cases where a rigid gravity retaining wall or a flexible cantilever retaining wall is constructed. Despite their structural simplicity, the seismic response of a wall (retaining even a single soil layer) is a rather complicated problem. The dynamic interaction between the wall and the retained soil is what makes that response so complicated, especially when material and/or geometry non-linearities are considered (PIANC (2001), Wu and Finn (1999)). The seismic response of various types of walls that support a single soil layer has been examined by a number of researchers in the past either experimentally, analytically, or numerically (Veletsos and Younan (1997), Iai (1998), Psarropoulos et al. (2005)). Depending on the assumed material behavior of the retained soil and the possible mode of the wall displacement, there exist two main categories of analytical methods used in the design of retaining walls against earthquakes: (a) the pseudo-static methods incorporating the limiting-equilibrium concept (Mononobe–Okabe type solutions), which assume yielding walls and rigid – perfectly plastic behavior of the retained soil (Okabe (1926), Mononobe and Matsuo (1929), Seed and Whitman (1970)), and (b) the elasticity-based solutions that regard the retained soil as a linear (visco-) elastic continuum (Veletsos and Younan (1997), Scott (1973), Wood (1975)).

According to an efficient simplification of the Mononobe-Okabe method, developed by Seed and Whitman (1970), the (maximum) normalized dynamic active earth force imposed on the wall is:

$$\overline{\Delta P}_{AE} = \frac{\Delta P_{AE}}{A\rho H^2} \approx 0.4 \tag{1.1}$$

where A is the peak base acceleration, ρ is the soil mass density, and H is the wall height. In the early '70s, the elastic solutions developed by Scott (1973) or Wood (1975) suggest that for the case of low-frequency (quasi-static) base motions, which refers to many practical problems, the normalized dynamic active earth force developed on a rigid fixed-base wall is $\overline{\Delta P}_{AE} \approx 1$. It is evident that this quantity is almost 2.5 times bigger than the proposal made by Seed and Whitman (1970). It has to be mentioned that, as it will be presented later on, this discrepancy may be even more intense when the fundamental frequency of the base excitation approaches that of the retained soil layer under one-dimensional (1–D) conditions, i.e.:

$$f_o = \frac{V_S}{4H} = \frac{\sqrt{G_{\max}/\rho}}{4H} \tag{1.2}$$

where V_S is the shear-wave velocity of the soil, and G_{max} is the corresponding small-strain shear modulus. However, the two aforementioned modes of wall-soil system behavior are rather extreme and in many cases fail to represent reality due to their unrealistic assumptions. The limiting-equilibrium solutions imply the capability of the system to develop relatively large displacements (geometric non-linearity) together with the formation of plastic zones (material non-linearity). In contrast, the elasticity-based solutions include only the potential geometric non-linearity by taking into account the wall flexibility and/or the wall foundation compliance (Veletsos and Younan (1997)). In some cases, such as bridge abutments, braced excavations, or basement walls, the existence of kinematic constraints on the wall motion is incompatible with the limiting-equilibrium concept, while on the other hand, the available elasticity-based solutions overlook the potential non-linear behavior of the retained soil, leading thus to over-conservative designs.

The objective of the present study is to examine more thoroughly the influence of material non-linearity on the dynamic distress of a wall retaining a single soil layer. For this purpose, two-dimensional numerical simulations are performed, utilizing the finite-element method in order to investigate some of the most important aspects of this complex phenomenon of dynamic non-linear wall-soil interaction. In order to “isolate” the effects of material non-linearity on the system response, the wall is considered to be rigid and fixed at its base. Apart from the dynamic earth pressures developed on the wall, emphasis is put on the soil amplification of the base acceleration. Note that seismic norms (such as the Eurocode EC8, or the Greek Seismic Code), being based on the limit-equilibrium methods, underestimate the role of the potential soil amplification. A parametric study has been performed in order to examine how the level of applied acceleration may affect the dynamic earth pressures induced on the retaining wall. Material non-linearity is taken into account in a simplistic, yet efficient way, through the use of an iterative equivalent-linear procedure in which strain-compatible shear modulus, G, and critical damping ratio, ξ, are used to describe the soil behavior within each iteration.

Dynamic response of any system depends on the seismic excitation characteristics (both in the time and in the frequency domain). However, in the present numerical study the excitations were limited on purpose to harmonic and simple pulses in order to examine more thoroughly the complex phenomena of non-linear dynamic wall-soil interaction. Results provide a clear indication of the direct dynamic interaction between a retaining wall and the retained soil, whilst potential soil non-linearity seems to increase the degree of complexity, being either beneficial or detrimental for the wall distress, depending on the circumstances. That fact justifies the necessity for a more elaborate consideration of these interrelated phenomena on the seismic design of retaining walls.

2. NUMERICAL MODELING

In order to examine the non-linear dynamic wall-soil interaction, two-dimensional (2-D) numerical simulations of a rigid fixed-base retaining system were conducted. The simulations were performed utilizing the finite-element code QUAD4M developed by Hudson et al. (1993), which performs dynamic non-linear analyses incorporating the well-known iterative equivalent-linear procedure. Each iteration includes: (a) a linear direct-integration dynamic analysis of the model, (b) the calculation of the maximum effective shear strain, γ_{eff}, for each element (calculated as a percentage of the maximum strain), and (c) the calculation of the strain-compatible shear modulus $G(\gamma_{eff})$ and critical damping ratio $\xi(\gamma_{eff})$ to be used in the next iteration, by means of $G/G_{\max}$ - γ and ξ - γ curves. The procedure is terminated when convergence in the values of G and ξ arises. The $G/G_{\max}$ - γ and ξ - γ curves used are characteristic of sandy soil material (Seed and Idriss (1970), Idriss (1990)).

In general, the soil material properties (G, ρ) and the wall height do not affect the dynamic pressures on the wall, as the wall flexibility is examined in relation to soil stiffness and the earth pressures are normalized with ρ and H (Veletsos and Younan (1997), Psarropoulos et al. (2005)). Therefore, all the analyses in the current investigation were performed considering an 8m-high wall. The retained soil layer is characterized by a relatively low small-strain shear-wave velocity V_S equal to 100m/s and a mass density of 1.8 Mg/m^3. The discretization of the retained soil was performed by four-node plane-strain quadrilateral elements. The model was adequately elongated so as to reproduce adequately the free-field conditions at the right-hand side of the model. The rigid wall was simulated by an extremely stiff column with linear elastic behavior. The simplifying assumption of no de-bonding or relative slip at the wall-soil interface was used.

The base of both the wall and the soil stratum were considered to be excited by a horizontal motion, assuming an equivalent force-excited system. The model was subjected to harmonic and Ricker pulses which allow for a better understanding and interpretation of the results. Furthermore, the results of harmonic excitations can be easily generalized for any real excitations via Fourier transformations. Moreover, various characteristic levels of peak base acceleration were used, aiming at the development of different degrees of material non-linearity.

3. LINEAR HARMONIC RESPONSE

The dynamic linear response of a single soil layer under 1-D conditions has been studied by many researchers, and analytical solutions for harmonic excitation can be found in the literature. In the case of harmonic excitation the response is controlled by the ratio f/f_o, where f is the dominant period of the excitation, and f_o the fundamental period of the soil layer. Therefore, the employed harmonic excitations had two characteristic frequencies: the first was set equal to the low-strain fundamental eigenfrequency of the soil layer ($f = f_o$), and the second pulse had frequency six times lower ($f = f_o/6$), approximating a quasi-static excitation.
In the examined model the fundamental frequency of the soil layer f_o is almost 3.1Hz (or equivalently, the fundamental period of the soil layer T_o is 0.32s). The duration of the sinusoidal pulse was such that steady state conditions were reached. In that case the maximum amplification factor (AF) for linear response is given by:

$$AF \cong \frac{2}{\pi\xi}\frac{1}{2n+1} \tag{3.1}$$

where ξ is the critical damping ratio and n the eigen-mode number. For first mode (n = 0) and ξ = 5%, AF is approximately equal to 12.7.

In this study the response of the soil layer under 1-D conditions is compared with the corresponding 2-D due to the existence of the wall. The presence of a retaining wall essentially imposes a vertical boundary condition, leading thus to a 2-D model. In addition, this model has a fundamental low-strain eigenfrequency slightly lower than the corresponding 1-D model, due to the fact that the existence of the rigid wall makes the model stiffer. However, the difference in the two values of eigenfrequency is considered negligible, as it is lower than 0.03 Hz. The distribution of the amplification factor (AF) on the surface of the backfill in the case of harmonic excitation at resonance ($f = f_o$) is plotted in Figure 1. It is evident that, for the rigid fixed-base wall examined, the motion in the vicinity of the wall is practically induced by the wall itself, and therefore, no amplification is observed (AF = 1). The amplification factor converges to its maximum value ($AF \approx 12.7$) at a distance of 10H from the wall, since at that distance 1-D conditions are present (*free-field motion*). Note that this distance was also calculated by Wood (1975), as the minimum distance required to eliminate the effects of the wall on the retained soil.
Figure 2 presents the height-wise distribution of the normalized induced dynamic earth pressures for the two harmonic excitations examined. It can be observed that when the fundamental frequency of the input motion f approaches that of the retained soil layer f_o, the normalized dynamic earth force is almost three times greater in the case of resonance, compared to the corresponding value in the case of quasi-static excitation, which is almost equal to unity.

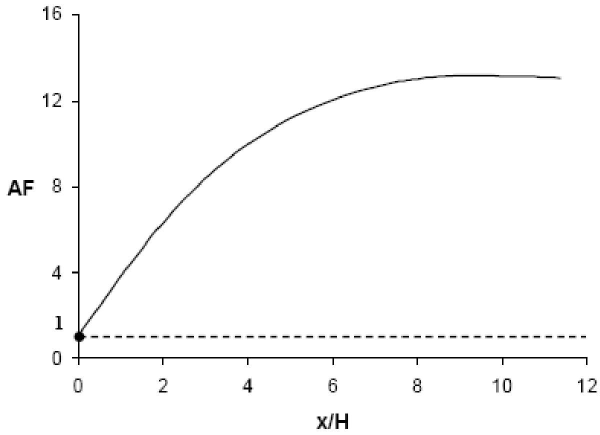

Figure 1 Distribution of the *AF* along the free surface of the backfill in the case of harmonic excitation at resonance ($f = f_o$). Note that *AF* is unity just behind the rigid wall examined, and along the backfill-base interface.

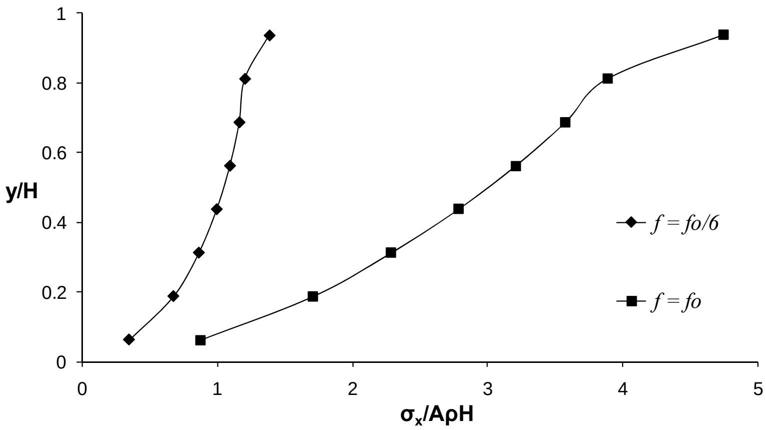

Figure 2 Distribution of the normalized induced dynamic earth pressures for the two harmonic excitations examined. Note that f_o is the fundamental low-strain eigenfrequency of the soil layer under 1-D conditions.

4. NON-LINEAR HARMONIC RESPONSE

The aforementioned results referring to the case of linear soil behavior are valid for very low levels of base input acceleration, when the induced strains remain small ($\gamma < 0.005\%$). However, when the maximum acceleration acting on the soil mass takes more realistic values the induced strains are substantially greater, and thus, the impact of material non-linearity (expressed by the G/G_{max} - γ and ξ - γ curves) become more evident. The wall-soil system behavior depends heavily, not only on the level of applied acceleration, but also on the f/f_o ratio, as it is justified by the subsequent results.

The distribution of the amplification factor on the surface of the backfill in the case of the harmonic excitation at resonance ($f = f_o$) is plotted in Figure 3, for five levels of peak base acceleration: 0.0001g (corresponding practically to a linear soil behavior), 0.12g, 0.24g, 0.36g, and 0.50g, covering a broad range of induced dynamic strains. Note that in the range of small shear strains the critical damping ratio, ξ, was set equal to 5%, instead of the much lower values of the curves proposed by Seed and Idriss (1970), in order to ensure that the theoretical amplification (e.g., $AF \approx 12.7$) for linear conditions is also numerically achieved for the lowest beak base acceleration case (0.0001g). As it was expected, increasing the degree of material non-linearity makes the system more flexible, thus decreases its fundamental frequency and leads to detuning. This phenomenon can be easily observed by examining the substantially reduced values of *AF*, for all levels (0.12g to 0.50g) of non-linear behavior, as shown in Figure 3.

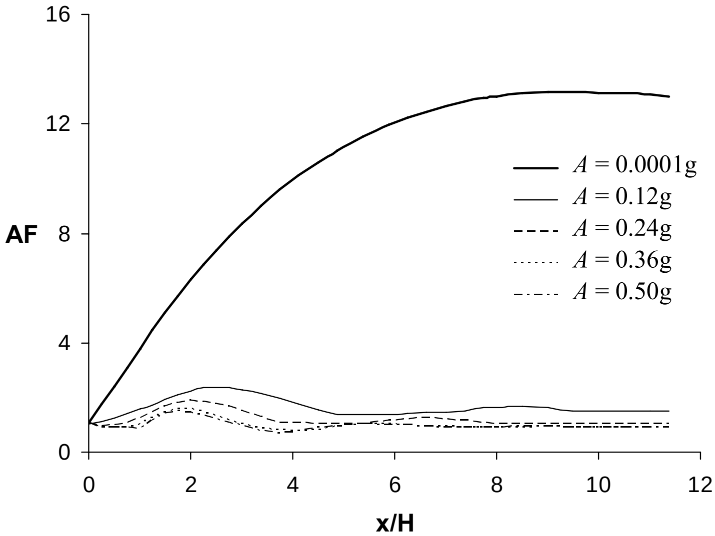

Figure 3 Distribution of the soil amplification factor (*AF*) along the surface of the backfill in the case of harmonic excitation with frequency f equal to the low-strain first eigenfrequency f_o.

Figure 4 depicts the height-wise distribution of the normalized induced dynamic earth pressures for the five levels of peak base acceleration examined in the case of the harmonic excitation with $f = f_o$. As the level of applied acceleration increases the dynamic earth pressures decrease. In particular, the normalized dynamic earth force on the wall reduces to values ranging from 0.60 to 0.90 (corresponding to A = 0.50g and 0.12g levels, respectively) compared to the previously calculated value of three for the linear soil behavior case. It is evident that for excitations having dominant frequency approaching the low-strain fundamental eigenfrequency of the retained soil layer, the material non-linearity seems to act in a beneficial way.

The case of quasi-static excitation is of greater interest. In Figure 5 the height-wise distribution of the normalized induced dynamic earth pressures is plotted for the case of the low-frequency harmonic excitation ($f = f_o/6$) for the five levels of peak base acceleration examined.

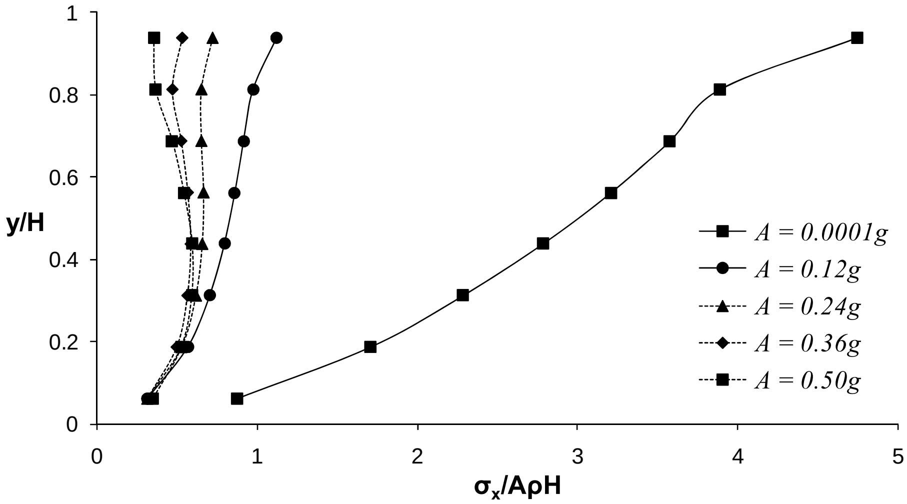

Figure 4 Height-wise distribution of the normalized induced dynamic earth pressures for the harmonic excitation with frequency f equal to the low-strain first eigenfrequency f_o.

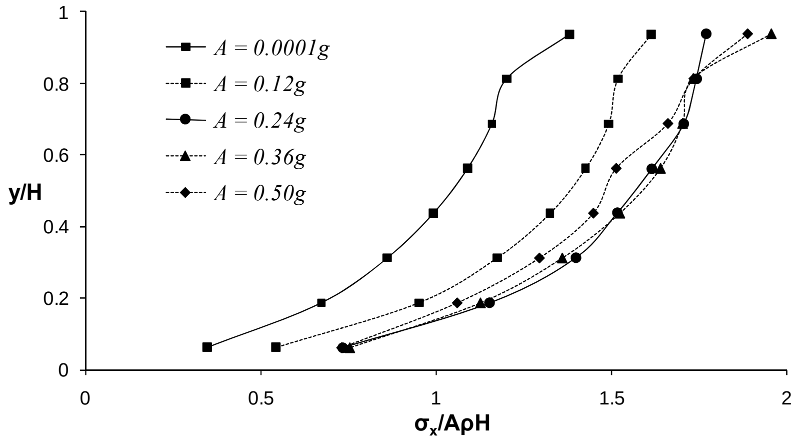

Figure 5 Distribution of the normalized induced dynamic earth pressures for the low-frequency harmonic excitation ($f = f_o/6$).

5. RESPONSE TO RICKER PULSE

As aforementioned, apart from harmonic excitations simple pulses have also been used in the present study. A simple Ricker pulse with central frequency $f_R = 2$Hz has been selected as a pulse excitation. Despite the simplicity of its waveform, this wavelet covers smoothly a broad range of frequencies up to nearly $3f_R$ (≈ 6Hz). The distribution of the normalized induced dynamic earth pressures in the case of the Ricker pulse excitation is plotted in Figure 6, for three of the levels of peak base acceleration examined. The pattern revealed in Figure 4 for the harmonic excitation is repeated in this case, due to the fact that the excitation pulse includes a broad range of frequencies close to the fundamental frequency of the retained soil layer ($f_o \approx 3$Hz). As a result, despite the lower pressures in this case, the system response is similar to that caused by the harmonic excitation at resonance.

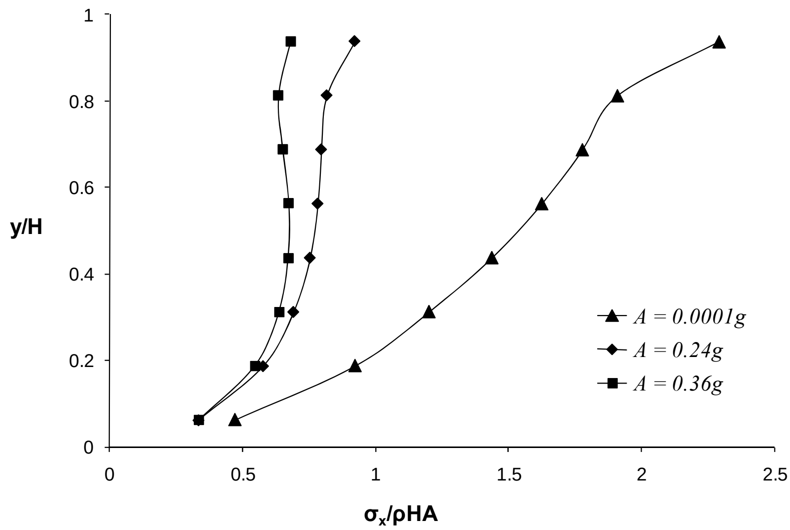

Figure 6 Distribution of the normalized induced dynamic earth pressures in the case of the Ricker pulse.

As this Ricker pulse covers smoothly the range of frequencies between 1 and 5Hz, it provides an efficient way to comprehend the effect of material non-linearity on the wall distress in the frequency domain as well. Figure 7 shows the variation of the *Pressure Amplification Factor* (*PAF*) as a function of frequency. The aforementioned parameter is defined as the ratio between the Fourier spectrum of the normalized induced dynamic earth force time history and the spectrum of the acceleration time history of a Ricker pulse excitation with unit peak value.

It is evident that in the case of linear soil behavior, *PAF* reaches its maximum value for frequencies close to the fundamental frequency of the retained soil layer. This result matches the value calculated previously in the case of linear harmonic response at resonance. Additionally, for low-frequency excitations, the value of *PAF* converges to that proposed by Scott (1973) and Wood (1975) as calculated previously. For the case of increased levels of peak base acceleration (i.e., A = 0.24g or 0.36g), the development of material non-linearity not only affects the maximum value of *PAF*, but also shifts the range of its maximum values towards lower frequencies.This phenomenon can be either beneficial or detrimental, depending on the predominant frequency of the input motion.

Finally, Figure 8 presents the maximum normalized dynamic earth force as a function of peak base acceleration for the three excitations examined. Note that in the same plot, the values proposed by Wood (1975) and Seed and Whitman (1970) are also included as references. It can be observed that in the case of linear response the wall distress is dominated by the frequency content of the excitation. More specifically, $\overline{\Delta P_{AE}}$ varies between the values of 1 and 3, being thus always higher than the standard bounding values adopted by the seismic norms. Nevertheless, as the degree of non-linearity increases the distress decreases substantially, ranging between the aforementioned Wood and M-O bounds in the cases of harmonic resonant and Ricker pulses.

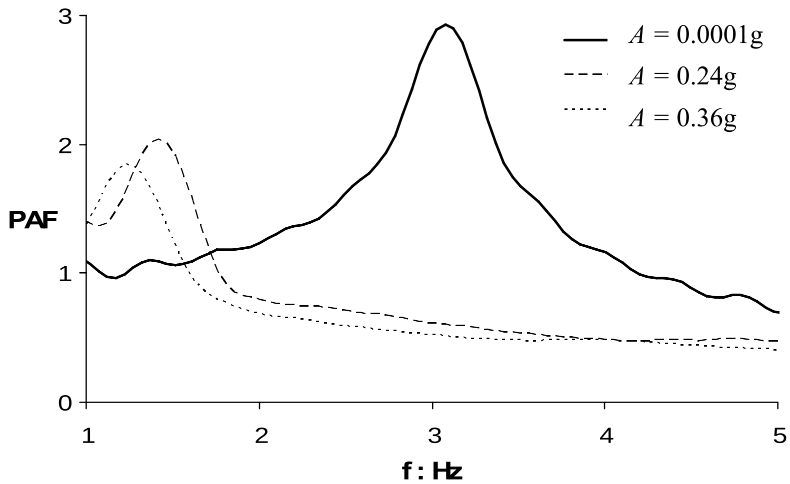

Figure 7 The Pressure Amplification Factors (*PAF*) calculated for the Ricker pulse excitation.

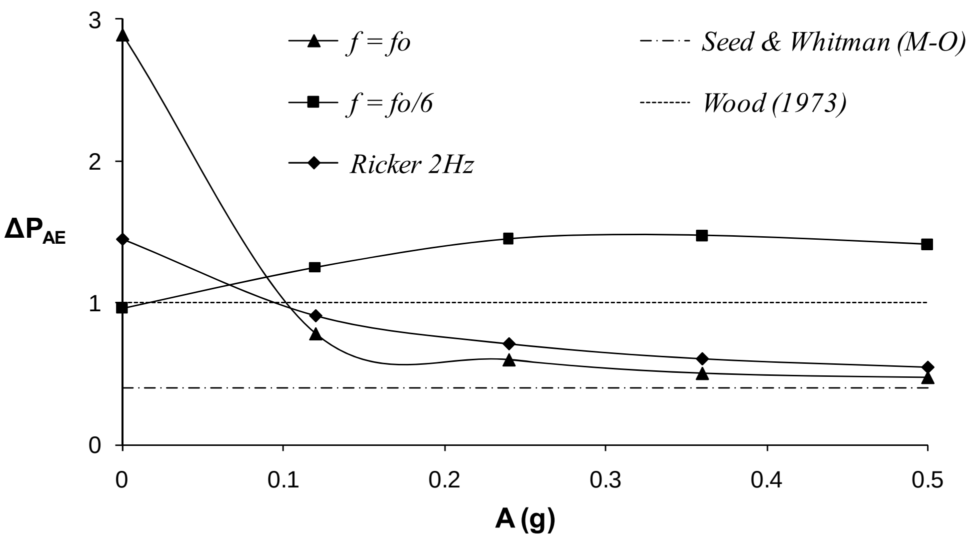

Figure 8 Maximum normalized dynamic earth force as a function of peak base acceleration A, for the three excitations examined. Graph also includes the proposals of Wood (1975) and Seed and Whitman (1970).

In contrast, the distress in the case of low-frequency harmonic excitation and non-linear response is always higher than the upper bound (Wood's solution), and is approximately 50% greater than the value of Wood's solution. An important conclusion resulting from Figure 8 is that for high values of the imposed acceleration the resulting force approximates in general the proposal of Seed and Whitman (1970), even though the limiting-equilibrium conditions (imposed by the static theory of Coulomb, or its pseudo-static extension of M-O) are not valid in the specific retaining system. In other words, the force acting on the back of a yielding retaining wall (resulting from the weight of a rigid wedge of soil above a planar failure surface, according to M-O theory) coincides with the force that acts on the back of a rigid fixed-base wall (resulting from the earth pressures of a yielding soil material).

6. CONCLUSIONS

The present study has examined how and to what extent the potential soil non-linearity, that a retained soil layer exhibits under moderate or severe seismic excitations can possibly affect the dynamic distress of a rigid fixed-base retaining wall, and the seismic response of the retained soil layer itself. It was found that soil non-linearity reduces in general the soil amplification of the retained soil and the dynamic earth pressures, leading thus to a lower wall distress. However, as soil non-linearity alters the eigenfrequencies of the wall-soil system, there exists (under certain circumstances) the possibility that increased non-linearity may lead to an amplified response. This phenomenon is more probable to occur when the frequency content of the excitation is narrow and concentrated around a fundamental frequency that is lower than the linear eigenfrequency of the soil layer. In any case, results provide a clear indication that the potential non-linearity increases the degree of complexity, being either beneficial or detrimental for the wall distress, depending on the circumstances. That fact justifies the necessity for a more elaborate consideration of these interrelated phenomena on the seismic design of retaining walls.

REFERENCES

Hudson, M.B., Idriss, I.M. and Beikae, M. (1993). QUAD4M: A computer program for evaluating the seismic response of soil-structures. *Center for Geotechnical Modeling, Department of CEE, Univ. of California*, Davis.

Iai, S. (1998). Seismic analysis and performance of retaining structures. in: Dakoulas, P., Yegian, M., Holtz, R.D. (Eds.), *Proc. Geotechnical Earthquake Engineering and Soil Dynamics III*, Geotechnical Special Publ. No. 75, Vol. 2, *ASCE*, Reston, VA, 1020–1044.

Idriss, I.M. (1990). Response of soft soil sites during earthquakes In: Duncan, J.M. (Ed.), *Proceedings*, *H. Bolton Seed Memorial Symposium*, **2,** 273-289.

Mononobe, N. and Matsuo, H. (1929). On the determination of earth pressures during earthquakes. *Proceedings of the World Engineering Congress*, Tokyo, Japan, **9,** paper 388.

Okabe, S (1926). General theory of earth pressures. *Journal of the Japan Society of Civil Engineering* **12:1**.

PIANC. (2001). International Navigation Association (PIANC): Seismic design guidelines for port structures. Balkema Publishers.

Psarropoulos, P.N., Klonaris, G. and Gazetas, G. (2005). Seismic earth pressures on rigid and flexible retaining walls. *Soil Dynamics and Earthquake Engineering* **25:7-10,** 795-809.

Scott, R.F. (1973). Earthquake-induced pressures on retaining walls. *Proceedings of the 5th World Conference on Earthquake Engineering*, **2,** 1611–1620.

Seed, H.B. and Idriss, I.M. (1970). Soil moduli and damping factors for dynamic response analyses. *Report EERC 70-10*, Earthquake Engineering Research Center, University of California, Berkeley, CA.

Seed, H.B. and Whitman, R.V. (1970). Design of earth retaining structures for dynamic loads. Proceedings of the Special Conference on Lateral Stresses in the Ground and Design of Earth Retaining Structures, ASCE, 103–147.

Veletsos, A.S. and Younan, A.H. (1997). Dynamic response of cantilever retaining walls. *ASCE Journal of Geotechnical and Geoenvironmental Engineering* **123:2,** 161–172.

Wood, J.H. (1975). Earthquake-induced pressures on a rigid wall structure. *Bulletin of New Zealand National Earthquake Engineering* **8,** 175–186.

Wu, G. and Finn, W.D.L. (1999). Seismic lateral pressures for design of rigid walls. *Canadian Geotechnical Journal* **36:3,** 509-522.